Crystal Structures of a Tetranucleating Macrocycle and its Dimanganese(III) Derivative, and Magnetism of the Latter*

Alison J. Edwards,[a] Bernard F. Hoskins,[a] Richard Robson,[a] Jenny C. Wilson,[a] Boujemaa Moubaraki[b] and Keith S. Murray[b]
[a] *School of Chemistry, University of Melbourne, Parkville, Victoria 3052, Australia*
[b] *Chemistry Department, Monash University, Clayton, Victoria 3168, Australia*

Condensation of 2,6-bis(aminomethyl)-4-methylphenol with 2,6-diformyl-4-methylphenol gave a macrocyclic tetra-Schiff base containing two of each component as the dihydrochloride salt $H_4L{\cdot}2HCl$, which has been studied by X-ray crystallography [triclinic, space group $P\bar{1}$ (no. 2), $a = 8.809(1)$, $b = 9.268(2)$, $c = 10.286(3)$ Å, $\alpha = 89.93(2)$, $\beta = 84.70(2)$, $\gamma = 72.18(2)°$; at convergence $R = 0.067$ and $R' = 0.060$ for 982 reflections with $I \geqslant 2.5\sigma(I)$]. The outstanding feature of the structure is that despite the overall dipositive charge resulting from protonation, the dialdehyde-derived oxygens are present as phenoxide anions. Crystals of composition $[Mn_2(H_2L)(\mu\text{-}O_2CMe)(\mu\text{-}OH)(MeOH)_2][ClO_4]_2{\cdot}2MeOH$ obtained from condensation of the dialdehyde and the diamine in the presence of Mn^{2+} and dioxygen were also studied by X-ray diffraction [monoclinic, space group $C2/c$ (no. 15), $a = 26.673(3)$, $b = 11.069(3)$, $c = 21.185(3)$ Å, $\beta = 127.44(1)°$; at convergence $R = 0.061$ and $R' = 0.061$ for 2102 reflections with $I \geqslant 3\sigma(I)$]. The two equivalent manganese centres have tetragonally distorted six coordinate ligand environments consistent with the high-spin d^4 configuration of the +III oxidation state, which is confirmed by the magnetic properties. The magnetic moment per Mn is 4.61 μ_B at room temperature falling to 1.8 μ_B at 10 K indicative of weak antiferromagnetic coupling with best-fit parameters obtained using a $-2JS_1{\cdot}S_2$ Heisenberg model of $g = 1.99(0.01)$, $J = -4.0(0.1)$ cm^{-1} and % monomer = 2.3(0.3).

Complexes in which a single ligand organises two or more metal centres into some predetermined arrangement may show unusual behaviour in a number of areas such as the multielectron oxidation or reduction of substrates, the trapping of substrates under unusual bonding circumstances and the activation of substrates to further reaction. Such molecules may in addition have applications in bioinorganic chemistry providing useful parallels with comparable metalloenzymes. Some Ni_4 and Zn_4 complexes of the tetranucleating tetra-Schiff-base ligand H_4L have been described previously.[1] We report here the crystal structure of the metal-free protonated ligand $H_4L{\cdot}2HCl$ and the synthesis, crystal structure and magnetic properties of a dimanganese(III) derivative, $[Mn_2(H_2L)(\mu\text{-}O_2CMe)(\mu\text{-}OH)(MeOH)_2][ClO_4]_2{\cdot}2MeOH$. This complex may serve as a useful model for the bacterial catalase enzymes for which the $Mn^{III,III}$–$Mn^{II,II}$ redox couple is thought to be the active state for H_2O_2 disproportionation.

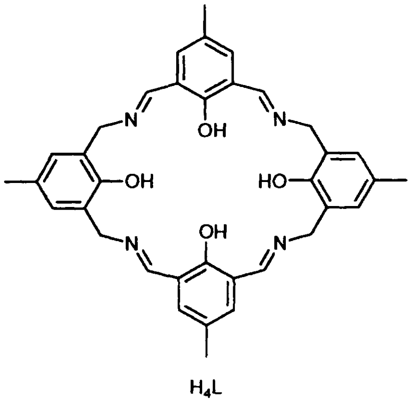

H_4L

Results and Discussion

Structure of $H_4L{\cdot}2HCl$.—The metal-free Schiff-base condensation of 2,6-bis(aminomethyl)-4-methylphenol with 2,6-diformyl-4-methylphenol has been described previously.[1b] In that report the product isolated was presumed to be $H_4L{\cdot}2HCl$. Subsequently, however, it was discovered that metal-templated condensation of the dialdehyde and diamine sometimes gave the macrocyclic 2:2 tetra-Schiff base and under other circumstances gave the macrocyclic 3:3 hexa-Schiff base.[2] It was therefore of some interest to ascertain whether the product of the metal-free condensation really was of the presumed 2:2 type or was the 3:3 or some other type.

Crystals suitable for X-ray studies were obtained directly from the condensation reaction mixture. The X-ray structural analysis confirms that the product is indeed the 2:2 tetra-Schiff-base macrocycle. The crystals contain H_6L^{2+} cations hydrogen bonded to chloride ions. The molecule is located around a crystallographic centre of inversion. The structure and atom numbering scheme are presented in Fig. 1. Atomic positional coordinates are given in Table 1 and selected bond distances and angles in Table 2.

The macrocycle consists of four separate, essentially internally planar blocks hinged together at the four methylene carbon centres, where pronounced twisting of one block relative to its attached neighbour occurs. The most outstanding feature of the molecule is that, despite the overall dipositive charge resulting from protonation, the dialdehyde-derived oxygens O(1) are present as *deprotonated* phenoxide anions. Hydrogen atoms are discernible, attached to all four imine nitrogen centres [N(1)–H(N1) 0.95(9), N(2)–H(N2) 0.89(9) Å] and to the two diamine-derived oxygen centres which are hydrogen bonded to the chloride ions [O(2)–H(O2) 1.02(9), H(O2) $\cdots$ Cl 2.02(9) Å].

---

* *Supplementary data available:* see Instructions for Authors, *J. Chem. Soc., Dalton Trans.*, 1994, Issue 1, pp. xxiii–xxviii.

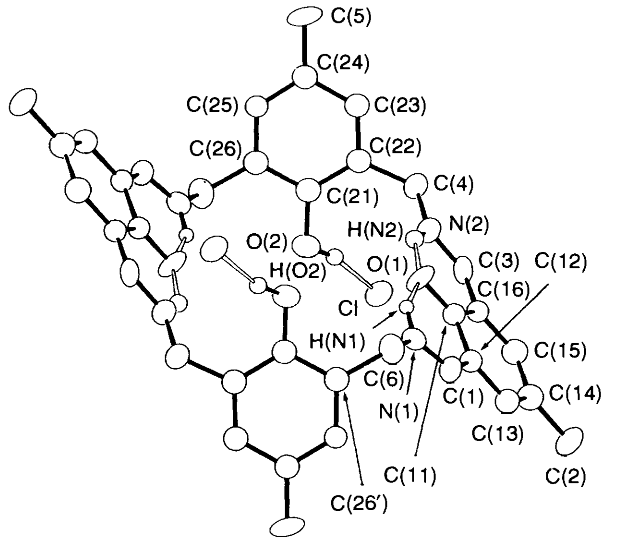

Fig. 1 Structure of $H_4L{\cdot}2HCl$ and atom numbering scheme used (hydrogen bonds are indicated)

Table 1 Fractional atomic coordinates for $H_4L{\cdot}2HCl$ with e.s.d.s in parentheses

Atom	*x*	*y*	*z*
Cl	0.2300(4)	0.0505(3)	0.0403(3)
O(1)	0.2114(8)	0.1990(6)	0.5637(6)
O(2)	0.1560(8)	0.3573(7)	0.1738(7)
N(1)	0.0139(9)	0.2404(9)	0.7833(8)
N(2)	0.389(1)	0.1343(9)	0.3369(8)
C(1)	0.027(1)	0.0997(9)	0.7673(9)
C(2)	0.170(1)	−0.4010(9)	0.542(1)
C(3)	0.369(1)	−0.0004(9)	0.3480(8)
C(4)	0.484(1)	0.1732(9)	0.2256(9)
C(5)	0.645(1)	0.644(1)	0.1650(9)
C(6)	−0.079(1)	0.337(1)	0.8941(9)
C(11)	0.202(1)	0.064(1)	0.5600(8)
C(12)	0.112(1)	0.0076(9)	0.6604(8)
C(13)	0.104(1)	−0.1412(9)	0.6519(8)
C(14)	0.183(1)	−0.243(1)	0.5496(9)
C(15)	0.271(1)	−0.190(1)	0.4533(9)
C(16)	0.282(1)	−0.042(1)	0.4562(9)
C(21)	0.278(1)	0.4202(9)	0.1712(9)
C(22)	0.432(1)	0.3402(9)	0.1992(8)
C(23)	0.548(1)	0.4135(9)	0.1966(8)
C(24)	0.516(1)	0.567(1)	0.1640(9)
C(25)	0.366(1)	0.641(1)	0.1359(8)
C(26)	0.243(1)	0.5741(9)	0.1401(8)
H(O2)	0.20(1)	0.25(1)	0.136(9)
H(N1)	0.08(1)	0.270(9)	0.717(8)
H(N2)	0.32(1)	0.19(1)	0.40(1)

Table 2 Selected interatomic distances (Å) and bond angles (°) for $H_4L{\cdot}2HCl$ with e.s.d.s given in parentheses

O(1)–C(11)	1.28(1)	O(2)–C(21)	1.37(1)
N(1)–C(1)	1.28(1)	N(1)–C(6)	1.47(1)
N(2)–C(3)	1.32(1)	N(2)–C(4)	1.47(1)
C(1)–C(12)	1.40(1)	C(2)–C(14)	1.51(1)
C(3)–C(16)	1.41(1)	C(4)–C(22)	1.51(1)
C(5)–C(24)	1.52(1)	C(6)–C(26′)	1.50(1)
C(11)–C(12)	1.44(1)	C(11)–C(16)	1.43(1)
C(12)–C(13)	1.41(1)	C(13)–C(14)	1.40(1)
C(14)–C(15)	1.38(1)	C(15)–C(16)	1.41(1)
C(21)–C(22)	1.39(1)	C(21)–C(26)	1.41(1)
C(22)–C(23)	1.39(1)	C(23)–C(24)	1.41(1)
C(24)–C(25)	1.35(1)	C(25)–C(26)	1.40(1)
N(1)–H(N1)	0.95(9)	N(2)–H(N2)	0.89(9)
O(2)–H(O2)	1.02(9)	Cl • • • H(O2)	2.02(9)
O(1) • • • H(N1)	1.86(8)	O(1) • • • H(N2)	1.8(1)
C(1)–N(1)–C(6)	124.6(6)	C(3)–N(2)–C(4)	122.6(6)
N(1)–C(1)–C(12)	125.0(7)	N(2)–C(3)–C(16)	123.6(6)
N(2)–C(4)–C(22)	112.8(6)	N(1)–C(6)–C(26′)	111.1(6)
O(1)–C(11)–C(12)	122.5(6)	O(1)–C(11)–C(16)	122.2(6)
C(1)–C(12)–C(11)	121.3(6)	C(1)–C(12)–C(13)	118.1(6)
C(2)–C(14)–C(13)	122.0(7)	C(2)–C(14)–C(15)	121.5(7)
C(3)–C(16)–C(11)	121.5(7)	C(3)–C(16)–C(15)	116.7(7)
O(2)–C(21)–C(22)	123.2(6)	O(2)–C(21)–C(26)	117.6(6)
C(4)–C(22)–C(21)	123.2(6)	C(4)–C(22)–C(23)	117.2(6)
C(6′)–C(26)–C(21)	120.6(6)	C(6′)–C(26)–C(25)	120.6(6)
C(5)–C(24)–C(23)	120.6(7)	C(5)–C(24)–C(25)	122.5(7)
H(N1)–O(1)–H(N2)	162(4)	H(N1)–O(1)–C(11)	99(2)
H(N2)–O(1)–C(11)	97(3)	Cl–H(O2)–O(2)	166(6)
H(N1)–N(1)–C(1)	110(3)	H(N1)–N(1)–C(6)	125(4)
O(1)–H(N1)–N(1)	142(6)	H(N2)–N(2)–C(3)	104(4)
H(N2)–N(2)–C(4)	132(4)	O(1)–H(N2)–N(2)	148(7)
O(1)–H(N2)–C(3)	104(5)	H(O2)–O(2)–C(21)	110(4)

(′) Refers to the transformation $-x, 1-y, 1-z$.

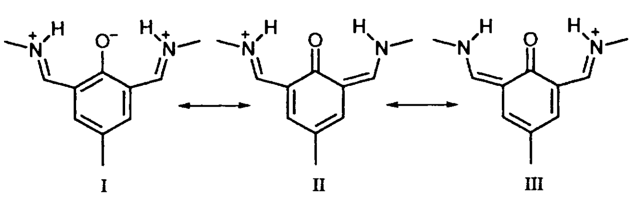

Remarkable bond lengths within the dialdehyde-derived residue are consistent with the deprotonation of the phenolic group which then acquires some quinonoid character. Thus, the O(1)–C(11) bond length of 1.28(1) Å is significantly shorter than the 1.37(1) Å observed for the comparable bond, O(2)–C(21), of the diamine-derived residue. The aromatic C–C bonds flanking the oxygen are significantly lengthened [C(11)–C(12) 1.44(1), C(11)–C(16) 1.43(1) Å] compared to the other aromatic C–C distances whilst the exocyclic C–C bonds, C(1)–C(12) and C(3)–C(16), are significantly shortened at 1.40(1) and 1.41(1) Å respectively. These distances are consistent with significant contribution of the quinonoid resonance structures **II** and **III**. It is well known that electron-withdrawing groups in the *ortho*- and *para*-positions increase the acidity of phenols. In the present example the phenolic group is flanked by two protonated imine substituents whose electron-withdrawing properties presumably are so extreme that the phenolic group remains unprotonated even when the molecule as a whole carries two additional protons. The imine hydrogens are hydrogen bonded to the aldehyde-derived phenoxide oxygen [O(1)• • •H(N1) 1.86(8), O(1) • • • H(N2) 1.8(1) Å].

Recently a very closely related structure was described[3] of a tetra-Schiff-base macrocyclic cation derived from the condensation of two moles of 2,6-diformyl-4-methylphenol with two moles of 1,3-diaminopropane in which the four imine nitrogens are protonated whilst two phenolic oxygen centres exist in the form of the phenolate anion. A related protonation pattern has been observed in the phenolic Schiff base, 2-[(4-diethylaminophenyl)iminomethyl]phenol in which the 'phenolic' hydrogen is disordered between a site where it is bonded to the phenolic oxygen and a site where it is bonded to the imine nitrogen.[4]

Structure and Magnetism of Solvated $[Mn_2(H_2L)(\mu\text{-}O_2CMe)(\mu\text{-}OH)(MeOH)_2][ClO_4]_2$.—In recent years great interest has been shown in the synthesis and properties of di- and poly-manganese complexes because they may serve as models for the manganese cluster in bacterial catalases, referred to above, and in the water-oxidising enzyme photosystem II. The latter system appears to involve at least two manganese centres probably bridged by O donors and co-ordinated also by other

O donors together with at most one or two N donors, EPR results strongly supporting a tetranuclear arrangement for the S_2 state.[5]

We have attempted to isolate Mn_4 complexes of L^{4-} related to the Ni_4 and Zn_4 derivatives reported previously,[1] but so far without success. Reaction of manganese(II) acetate with 2,6-bis(aminomethyl)-4-methylphenol and 2,6-diformyl-4-methylphenol in the presence of lithium acetate and sodium perchlorate in boiling methanol followed by saturation of the solution with dioxygen after it had cooled to room temperature, gave brown crystals of composition $[Mn_2(H_2L)(\mu\text{-}O_2CMe)(\mu\text{-}OH)(MeOH)_2][ClO_4]_2\cdot2MeOH$ characterised, as described below, by X-ray crystallography. After being dried in vacuum at room temperature (elevated temperatures were avoided because of the potentially explosive character of this perchlorate salt) and then being re-exposed to the atmosphere the solid had the composition $[Mn_2(H_2L)(\mu\text{-}O_2CMe)(\mu\text{-}OH)(MeOH)_2][ClO_4]_2\cdot2H_2O$.

The X-ray diffraction study revealed cations of composition $[Mn_2(H_2L)(\mu\text{-}O_2CMe)(\mu\text{-}OH)(MeOH)_2]^{2+}$ together with two perchlorate anions and lattice methanol. A view of the structure of the cation together with the atom numbering scheme is given in Fig. 2. Atomic coordinates are given in Table 3 and selected interatomic distances and angles in Table 4.

The cation is situated around a crystallographic two-fold axis of symmetry passing through the bridging hydroxide [O(4)] and through the carbon–carbon bond of a bridging acetate [C(7)–C(8)].

Each manganese atom has a tetragonally distorted six-co-ordinate environment indicative of the +III oxidation state with a high-spin d^4 configuration, for which such Jahn–Teller distortions are common; magnetic properties, discussed below confirm the +III oxidation state. The tetragonally elongated bonds are those to co-ordinated methanol [Mn(1)–O(5) 2.338(7) Å] and to the bridging acetate [Mn(1)–O(3) 2.143(6) Å], the remaining co-ordinate bonds to donors provided by the macrocyclic ligand and to the bridging hydroxide being typical for Mn^{III} [Mn(1)–O(1) 1.864(9),

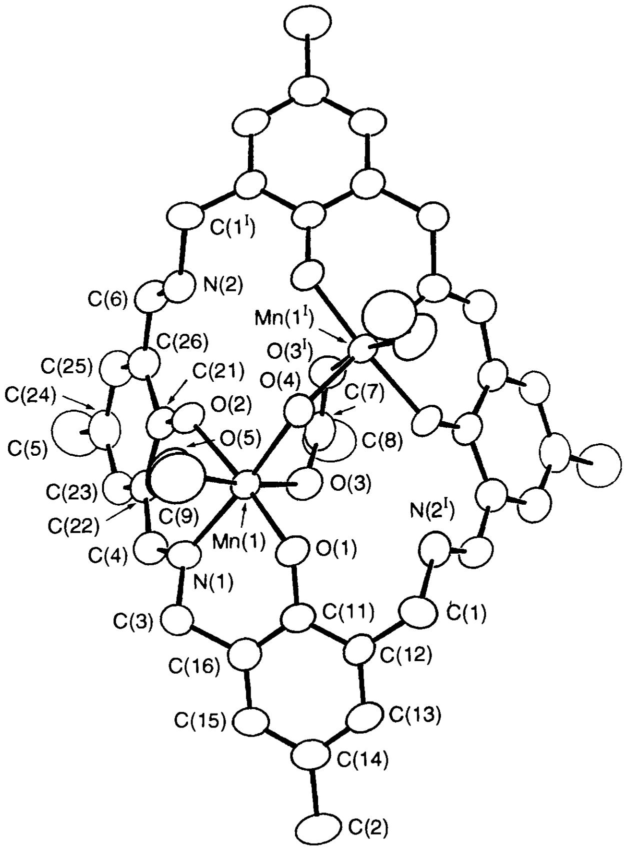

Fig. 2 The atomic arrangement and numbering scheme of the cation $[Mn_2(H_2L)(\mu\text{-}O_2CMe)(\mu\text{-}OH)(MeOH)_2]^{2+}$

Table 3 Fractional atomic coordinates for the non-hydrogen atoms of $[Mn_2(H_2L)(\mu\text{-}O_2CMe)(\mu\text{-}OH)(MeOH)_2][ClO_4]_2\cdot2MeOH$ with e.s.d.s given in parentheses

Atom	*x*	*y*	*z*
Mn(1)	0.4334(1)	0.1472(1)	0.1487(1)
O(1)	0.4692(3)	0.0918(5)	0.1011(3)
O(2)	0.3892(2)	0.1924(5)	0.1907(3)
O(3)	0.4801(3)	0.3189(5)	0.1862(3)
O(4)	0.5000	0.0691(7)	0.2500
O(5)	0.6265(3)	−0.0286(6)	0.3845(4)
N(1)	0.3596(3)	0.2172(7)	0.0444(4)
N(2)	0.4037(3)	0.1787(6)	0.3228(4)
C(1)	0.5745(4)	0.1093(8)	0.1015(5)
C(2)	0.4338(5)	0.2719(9)	−0.1746(6)
C(3)	0.3446(4)	0.1620(8)	−0.0297(5)
C(4)	0.3260(4)	0.3058(7)	0.0382(5)
C(5)	0.2601(5)	0.6366(8)	0.1329(6)
C(6)	0.3726(4)	0.2768(7)	0.3023(5)
C(7)	0.5000	0.3728(1)	0.2500
C(8)	0.5000	0.5105(1)	0.2500
C(9)	0.6129(6)	−0.1502(10)	0.3901(7)
C(11)	0.4598(4)	0.1387(7)	0.0350(4)
C(12)	0.5108(4)	0.1487(7)	0.0331(5)
C(13)	0.5012(4)	0.1911(7)	−0.0349(5)
C(14)	0.4421(4)	0.2266(8)	−0.1012(5)
C(15)	0.3919(4)	0.2178(7)	−0.0978(5)
C(16)	0.4003(4)	0.1735(7)	−0.0311(5)
C(21)	0.3589(4)	0.2939(7)	0.1751(5)
C(22)	0.3294(4)	0.3588(8)	0.1028(5)
C(23)	0.2989(4)	0.4676(8)	0.0910(5)
C(24)	0.2936(4)	0.5167(8)	0.1469(5)
C(25)	0.3193(4)	0.4513(8)	0.2159(5)
C(26)	0.3512(4)	0.3407(7)	0.2314(5)
Cl(1)	0.2355(1)	0.5165(2)	0.8287(2)
O(11)	0.2413(5)	0.5291(10)	0.8999(5)
O(12)	0.1708(5)	0.5467(9)	0.7740(6)
O(13)	0.2473(5)	0.3992(8)	0.8214(7)
O(14)	0.2744(5)	0.5995(8)	0.8304(7)
O(MeOH)	0.0708(7)	0.0144(12)	0.4871(9)
C(MeOH)*	0.1126(10)	0.1211(15)	0.5016(12)
C(MeOH)*	0.0048(11)	−0.0461(15)	0.4136(13)

* The C atom of the lattice methanol C(MeOH) is disordered over two sites.

Table 4 Selected interatomic distances (Å) and bond angles (°) for $[Mn_2(H_2L)(\mu\text{-}O_2CMe)(\mu\text{-}OH)(MeOH)_2][ClO_4]_2\cdot2MeOH$ with e.s.d.s given in parentheses.

Mn(1)–O(1)	1.864(9)	Mn(1)–O(2)	1.925(8)
Mn(1)–O(3)	2.143(6)	Mn(1)–O(4)	1.968(4)
Mn(1)–O(5)	2.338(7)	Mn(1)–N(1)	2.017(6)
O(1)–C(11)	1.366(12)	O(2)–C(21)	1.304(10)
N(1)–C(3)	1.495(14)	N(1)–C(4)	1.280(13)
N(2)–C(1)	1.538(13)	N(2)–C(6)	1.272(11)
C(7)–C(8)	1.524(16)	Mn(1)–Mn(1^I)	3.535(2)
O(1)–Mn(1)–O(3)	96.8(3)	O(1)–Mn(1)–O(4)	91.5(3)
O(1)–Mn(1)–O(5)	92.6(4)	O(1)–Mn(1)–N(1)	90.8(4)
O(2)–Mn(1)–O(3)	88.8(3)	O(2)–Mn(1)–O(4)	90.6(3)
O(2)–Mn(1)–O(5)	81.8(3)	O(2)–Mn(1)–N(1)	86.7(3)
O(3)–Mn(1)–O(4)	92.8(3)	O(4)–Mn(1)–O(5^I)	87.8(3)
O(3)–Mn(1)–N(1)	91.5(4)	O(3)–Mn(1)–O(5^I)	170.6(4)
O(4)–Mn(1)–N(1)	174.9(3)	O(5^I)–Mn(1)–N(1)	87.5(4)
Mn(1)–O(4)–Mn(1^I)	127.9(3)	Mn(1)–N(1)–C(3)	117.0(6)
Mn(1)–N(1)–C(4)	124.2(6)	C(3)–N(1)–C(4)	118.8(7)
N(1)–C(3)–C(16)	110.4(7)	O(3)–C(7)–O(3^I)	123.6(5)
O(3)–C(7)–C(8)	118.2(5)	O(3^I)–C(7)–C(8)	118.2(5)

Symmetry operation: I $1 - x, y, \frac{1}{2} - z$.

Mn(1)–O(2) 1.925(8), Mn(1)–O(4) 1.968(4), Mn(1)–N(1) 2.017(6) Å]. Angles at manganese (see Table 4) range from 81.8(3) to 96.8(3)°. The co-ordination plane around Mn(1) consisting of O(1), O(2), N(1) and O(4) is inclined at a dihedral angle of 58.5° to the analogous plane around Mn(1^I).

Assignment of the +III oxidation state to both Mn centres is supported by bond valence sum (BVS) analysis,[6] an empirical procedure using metal–ligand distances to determine oxidation states which has recently been applied to the manganese centres in photosystem II.[7] Application of the BVS method to the dimanganese complex described here gives an oxidation state of 3.0.

The Mn(1)–O(4)–Mn(1^I) angle at the bridging hydroxide centre is 127.9(3)°. As is apparent in Fig. 2 the bridging acetate is twisted relative to the Mn(1)–O(4)–Mn(1^I) plane such that the symmetry related oxygen atoms are 0.574 Å on opposite sides of that plane.

The macrocyclic ligand consists essentially of four rigid, almost planar blocks, hinged together at the four methylene carbons where pronounced twisting of one block relative to its attached neighbour occurs; one type of block is the diamine-derived residue consisting of C(1), C(11)–C(16), C(3), C(2) and O(1) and the other is the di-Schiff-base component consisting of C(3), N(1), C(4), C(21)–C(26), C(5), O(2), C(6), N(2) and C(1^I). In its complexes the L^{4-} ligand commonly adopts a bowl-like conformation with all four C_6 rings inclined on the same side of the average plane defined by the four nitrogen atoms. As can be seen in Fig. 2 where the molecular bowl is viewed from its underside, the dialdehyde-derived C_6 rings [C(21)–C(26) and C(21^I)–C(26^I)] are considerably more steeply inclined (dihedral angle between the two 120.1°) than the diamine-derived C_6 rings (dihedral angle between the two 136.9°). This difference in inclination is reflected in the Me ··· Me separations across the molecule [C(2) ··· C(2^I) 16.09(2), C(5) ··· C(5^I) 10.55(2) Å]. No evidence was forthcoming from the diffraction data concerning the location of the two protons in the H_2L^{2-} component but on the basis of comparison with $H_4L{\cdot}2HCl$ above, attachment to the unco-ordinated nitrogens N(2) and N(2^I) seems very likely.

The magnetic moment of the $2H_2O$ solvated form of the Mn complex is 4.61 μ_B, per Mn, at room temperature. The reduction in μ_{Mn} from the spin-only $S = 2$ value of 4.87 μ_B is symptomatic of weak intramolecular antiferromagnetic coupling occurring between the Mn^{III} ions in the binuclear units, each ion possibly also displaying a small zero-field splitting (z.f.s.) of its $^5B_{1g}$ ligand-field ground state (see later). The μ_{eff} values decrease gradually with decreasing temperature to a value of 1.8 μ_B at 10 K. The corresponding χ_{Mn} *versus* temperature plot, shown in Fig. 3, reaches a plateau between 25 and 10 K. In combination with the decreased χ_{Mn} value at room temperature, and a detailed knowledge of the simultaneous effects of z.f.s. and exchange coupling at low temperatures in $S = 2$ systems,[8] we are convinced that the plateau represents a maximum, due to weak antiferromagnetic coupling, superimposed on which is a Curie component arising from a small fraction of monomer impurity, the latter a phenomenon commonly encountered in the most crystalline of samples. Indeed, a good-fit to the data can be obtained assuming a $-2JS_1{\cdot}S_2$ Heisenberg coupling model with best-fit values of $g = 1.99 \pm 0.01$, $J = -4.0 \pm 0.1$ cm^{-1} and %monomer = 2.3 ± 0.3. This is the fit shown in Fig. 3. The errors in the parameters were deduced by making small and systematic variations in each parameter and recognising that, whilst all three parameters influenced the size of the calculated susceptibility at a particular temperature, the J value responded most sensitively to the curvature and position of the susceptibility maximum. The z.f.s. was assumed zero in this model. In axially elongated Mn^{III} Schiff-base complexes of the present general type, the $^5B_{1g}$ ground state will, in principle, show z.f.s. such that the axial parameter, D, is negative in sign.[8] A smaller rhombic splitting (E) might also be anticipated. Comparison to our related previous work,[8,9] in combination with attempted fitting of the χ_{Mn}/T data by use of matrix diagonalisation methods, gives an estimate of D that is less than 0.5 cm^{-1}. It is actually possible to calculate a plateau in susceptibility at very low temperatures with J set at zero, but the D value needed to do this is unrealistically high, at 50 cm^{-1}, and the agreement with the observed χ_{Mn} values is very poor. A more precise evaluation of D would require the measurement and analysis of single-crystal data and/or of variable field/variable temperature data, the so-called multifield saturation magnetisation method.[8,10] These were deemed not to be necessary in the present study.

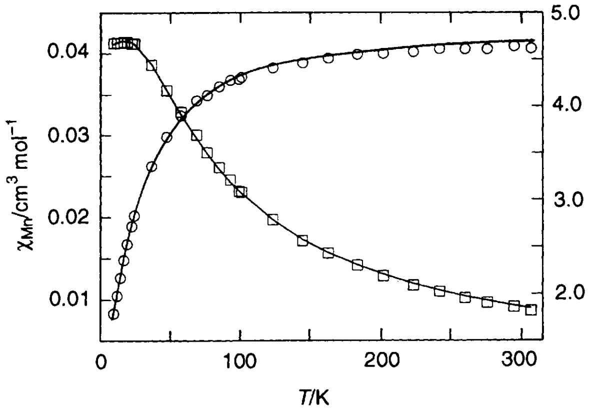

Fig. 3 Plots of μ_{Mn}(○) and χ_{Mn}(□) *versus* temperature for $[Mn_2(H_2L)(\mu\text{-}O_2CMe)(\mu\text{-}OH)(MeOH)_2][ClO_4]_2{\cdot}2H_2O$. The solid line is that calculated using a $-2JS_1{\cdot}S_2$ model with $g = 1.99$ and $J = -4.0$ cm^{-1}, %monomer = 2.3, where $S_1 = S_2 = 2$

The small negative value of J observed here is typical of the weak coupling noted in various (μ-carboxylato)$_y$, μ-X-bridged $Mn^{III}Mn^{III}$ systems in which y can be 1 or 2 and X can be O^{2-}, OR^- *etc.* In such compounds the J values have been found to be weakly antiferro- or ferro-magnetic in overall sign. There appears to be little correlation to date, with the precise nature of the bridging atoms or with the 'end' groups, the latter commonly being provided by chelating ligands of 2,2′-bipyridine, 1,4,7-triazacyclononane, hydrotris(pyrazolyl)borate or binucleating Schiff-base types.[5c,11,12] The present doubly bridged μ-O_2CMe, μ-OH combination is quite rare for $Mn^{III}Mn^{III}$. By analogy to $Fe^{III}(\mu\text{-}O_2CMe)_y(\mu\text{-}OH)Fe^{III}$ *versus* $Fe^{III}(\mu\text{-}O_2CMe)_y(\mu\text{-}O)Fe^{III}$ combinations[13] one might expect a related increase in the negative sign of J when OH^- is replaced by O^{2-}, *i.e.* more strongly antiferromagnetic. This is not the case in $Mn^{III}Mn^{III}$. Interestingly, in work related to ours,[14] Kitajima and co-workers[15] have recently obtained a doubly bridged compound $[L'Mn^{II}(\mu\text{-}O_2CMe)(\mu\text{-}OH)Mn^{II}L']$ [L′ = hydrotris(3,5-diisopropylpyrazol-1-yl)borate], which, on oxidation with either O_2 or H_2O_2 produces two μ-oxo species, *viz.* $[L'Mn^{III}(\mu\text{-}O_2CMe)(\mu\text{-}O)Mn^{III}L']^+$ and $[L'Mn^{III}(\mu\text{-}O_2CMe)(\mu\text{-}O)_2Mn^{IV}L']$. These species were thought to form *via* μ-(O_2)-bridged intermediates and the first was proposed as a model for manganese catalase. Since it seems likely that a $Mn^{II}(\mu\text{-}O_2CMe)(\mu\text{-}OH)Mn^{II}$ precursor complex is formed first in the present synthesis, the subsequent isolation of a μ-OH rather than a μ-O product is presumably related to the use of different solvents which, together with the ligand milieu used could well affect the effective pH of the medium. Further addition of base to the present complex would presumably lead to the formation of the (μ-O_2CMe)(μ-O) analogue. Finally we note that the crystal structure recently published[16] of the diiron protein methane monooxygenase contains the same (μ-O_2CMe)(μ-OH) bridging system and a very similar metal environment as that found in the present complex.

Experimental

The compound $H_4L{\cdot}2HCl$ was prepared as described previously.[1]

Preparation of $[Mn_2(H_2L)(\mu-O_2CMe)(\mu-OH)(MeOH)_2][ClO_4]_2\cdot 2H_2O$.—The compounds $Mn(O_2CMe)_2\cdot 4H_2O$ (0.31 g, 1.3 mmol) and $Li(O_2CMe)\cdot 2H_2O$ (0.31 g, 3.0 mmol) were dissolved together in methanol (10 cm^3) and then added to a methanolic solution (10 cm^3) of 2,6-diformyl-4-methylphenol (0.13 g, 0.79 mmol). 2,6-Bis(aminomethyl)-4-methylphenol (0.16 g, 0.78 mmol) dissolved in boiling methanol (10 cm^3) was added quickly to the above solution. The resultant brown solution was heated under reflux for 30 min and then $NaClO_4$ (0.52 g, 4.2 mmol) was added, initiating precipitation of an amorphous brown solid. After removal of the precipitate by filtration dioxygen was bubbled into the filtrate for 1.5 h. The solution was then concentrated at atmospheric pressure to 5 cm^3. Upon cooling, the solution deposited brown crystals of $[Mn_2(H_2L)(\mu-O_2CMe)(\mu-OH)(MeOH)_2][ClO_4]_2\cdot 2MeOH$, which were collected, washed with methanol (10 cm^3) and dried *in vacuo* at room temperature. Drying above room temperature was not attempted because of the potentially explosive character of this perchlorate salt. Yield: 0.05 g. After exposure to the atmosphere the solid had a composition consistent with the formulation $[Mn_2(H_2L)(\mu-O_2CMe)(\mu-OH)(MeOH)_2][ClO_4]_2\cdot 2H_2O$ (Found: C, 44.8; H, 4.8; N, 5.2. $C_{40}H_{48}Cl_2Mn_2N_4O_{19}$ requires C, 44.9; H, 4.5; N, 5.2%).

Crystal Structure Analyses.—Colourless crystals of $H_4L\cdot 2HCl$ and brown crystals of $[Mn_2(H_2L)(\mu-O_2CMe)(\mu-OH)(MeOH)_2][ClO_4]_2\cdot 2MeOH$ were grown directly from their reaction mixtures. A single crystal was sealed in a Lindeman glass tube with a small amount of solvent to prevent crystal deterioration.

Crystal data and details pertaining to the data collections are given in Table 5. Intensity data were measured at 294 K using an Enraf-Nonius CAD-4F single-crystal, automatic diffractometer with monochromated Mo-Kα radiation (λ = 0.710 69 Å) and the ω–2θ scan technique. Accurate cell dimensions and the orientation matrix were determined by a least-squares procedure using the angular settings of 25 carefully centred reflections. Corrections for Lorentz, polarisation and absorption effects were applied,[17] but no correction was made for extinction. The scattering factors used for C, H, N, O and Cl were those incorporated into the SHELX 76 program.[18] The values for manganese were corrected for real and imaginary dispersion and were taken from ref. 17. The positions of the majority of the non-hydrogen atoms for $H_4L\cdot 2HCl$ and the manganese atoms for $[Mn_2(H_2L)(\mu-O_2CMe)(\mu-OH)(MeOH)_2][ClO_4]_2\cdot 2MeOH$ were indicated by the SHELXS 86 program[19] using the direct-method routine. The remaining non-hydrogen atoms were located in subsequent difference maps produced by SHELX 76.[18] Both structures were refined using full-matrix least squares with anisotropic thermal parameters applied to all non-hydrogen atoms excluding those of the lattice methanol for $[Mn_2(H_2L)(\mu-O_2CMe)(\mu-OH)(MeOH)_2][ClO_4]_2\cdot 2MeOH$. Difference maps indicated the positions of all the hydrogen atoms. All hydrogen atoms except those associated with solvent methanol were however included in the scattering model at geometrically estimated positions (C–H 1.08, N–H 1.01 Å). The refinement was continued until convergence to yield the values of R, R' and g listed in Table 5, together with the values of maximum residual electron densities. Crystallographic diagrams were prepared using ORTEP.[20]

Additional material available from the Cambridge Crystallographic Data Centre comprises H-atom coordinates, thermal parameters and remaining bond lengths and angles.

Magnetic Measurements.—Magnetic susceptibility measurements were made on an Oxford Instruments Faraday magnetometer details of which, including measurement errors have been given previously.[8] Data were collected on the neat microcrystalline sample after it had been exposed to the atmosphere (see above). A main field of 5000 G and a gradient field of 1000 G cm^{-1} (G = 10^4 T) was employed. Crystalline alignment effects, sometimes noted in neat powdered samples of Mn^{III} complexes,[8] were checked to be absent.

Table 5 Crystal data and details of the crystal structure determinations

Formula	$C_{36}H_{38}Cl_2N_4O_4$	$C_{42}H_{50}Cl_2Mn_2N_4O_{19}$
M	661.63	1095.48
Crystal system	Triclinic	Monoclinic
Space group	$P\bar{1}$ (no. 2)	$C2/c$ (no. 15)
a/Å	8.809(1)	26.673(3)
b/Å	9.268(2)	11.069(3)
c/Å	10.286(3)	21.185(3)
α/°	89.93(2)	
β/°	84.70(2)	127.44(1)
γ/°	72.18(2)	
U/Å^3	795.7	4966
D_c/g cm^{-3}	1.38	
D_m/g cm^{-3}	1.37(2)	*
Crystal dimensions (mm from the centroid)	±(001), 0.071 ±(100), 0.071 ±(100), 0.143	±(100), 0.271 ±(010), 0.178 ±(10$\bar{1}$), 0.221
F(000)	348	2359
μ(Mo-Kα)/cm^{-1}	2.06	6.36
Absorption correction (min., max. transmission coefficients)	0.9847, 0.9841	0.761, 0.811
2θ range/°	2–45	2–45
Range of h, k, l	$-1 \leqslant h \leqslant 9$ $-10 \leqslant k \leqslant 10$ $-11 \leqslant l \leqslant 11$	$-1 \leqslant h \leqslant 28$ $0 \leqslant k \leqslant 11$ $-22 \leqslant l \leqslant 22$
Total no. of reflections	3248	3487
No. of unique reflections	2078	3236
R_{int}	0.031	0.013
No. of unique reflections used in refinement	982 [$I \geqslant 2.5\,\sigma(I)$]	2102 [$I \geqslant 3\sigma(I)$]
Function minimised	$\Sigma w(\lvert F_o\rvert - \lvert F_c\rvert)^2$	$\Sigma w(\lvert F_o\rvert - \lvert F_c\rvert)^2$
Weighting scheme parameters in $w = [k/\sigma^2(F_o) + gF_o^2]$	$k = 2.272$ $g = 0.0005$	$w = 1.00$
No. of variables	170	332
Final R	0.067	0.061
Final R'	0.060	0.061
Max. shift/e.s.d. for non-hydrogen atoms	0.009	
Goodness of fit, S	1.46	5.18
Maximum residual electron density/e Å^{-3}	0.32	0.77

* The crystals were very sensitive to loss of solvent making the density measurement impossible.

Acknowledgements

The authors thank the Australian Research Council for support and Dr. A. Markiewicz for help with the magnetic study.

References

1 (*a*) M. Bell, A. J. Edwards, B. F. Hoskins, E. H. Kachab and R. Robson, *J. Chem. Soc., Chem. Commun.*, 1987, 1852; (*b*) M. Bell, A. J. Edwards, B. F. Hoskins, E. H. Kachab and R. Robson, *J. Am. Chem. Soc.*, 1989, **111**, 3603; (*c*) M. Bell, A. J. Edwards, B. F. Hoskins, E. H. Kachab, A. Markiewicz, K. S. Murray and R. Robson, *Inorg. Chem.*, 1992, **31**, 3585.

2 B. F. Hoskins, R. Robson and P. Smith, *J. Chem. Soc., Chem. Commun.*, 1990, 488.

3 A. J. Atkins, A. J. Blake and M. Schröder, 29th International Conference on Coordination Chemistry, Lausanne, July 1992, Abstract P678.

4 G. P. Moloney, R. W. Gable, M. N. Iskander, D. J. Craik and M. F. Mackay, *Aust. J. Chem.*, 1990, **43**, 99.

5 (*a*) R. D. Britt, J. L. Zimmermann, K. Sauer and M. P. Klein, *J. Am. Chem. Soc.*, 1989, **111**, 3522; (*b*) D. H. Kim, R. D. Britt, M. P. Klein

and K. Sauer, *J. Am. Chem. Soc.*, 1990, **112**, 9389; (*c*) K. Wieghardt, *Angew. Chem., Int. Ed. Engl.*, 1989, **28**, 1153.

6 I. D. Brown and D. Altermatt, *Acta Crystallogr., Sect. B*, 1985, **41**, 244.

7 H. H. Thorp, *Inorg. Chem.*, 1992, **31**, 1585.

8 B. J. Kennedy and K. S. Murray, *Inorg. Chem.*, 1985, **24**, 1552.

9 K. Bertoncello, G. D. Fallon, K. S. Murray and E. R. T. Tiekink, *Inorg. Chem.*, 1991, **30**, 3562.

10 H. G. Jang, M. P. Hendrick and L. Que, jun., *Inorg. Chem.*, 1993, **32**, 911.

11 G. C. Dismukes, in *Bioinorganic Catalysis*, ed. J. Reedijk, Marcel Dekker, Amsterdam, 1993, p. 317.

12 M. Sivaraja, J. S. Phio, J. Lary and G. C. Dismukes, *J. Am. Chem. Soc.*, 1989, **111**, 3221.

13 D. F. Kurtz, jun., *Chem. Rev.*, 1990, **90**, 585.

14 J. C. Wilson, Ph.D. Thesis, University of Melbourne, 1990.

15 S. Imai, M. Osawa, Y. Moro-Oka and N. Kitajima, *J. Inorg. Biochem.*, 1993, **51**, 195.

16 A. C. Rozenzwerg, C. A. Frederick, S. J. Lippard and P. Nordlund, *Nature (London)*, 1993, **366**, 537.

17 *International Tables for X-Ray Crystallography*, eds. J. A. Ibers and W. C. Hamilton, Kynoch Press, Birmingham, 1974, vol. 4.

18 G. M. Sheldrick, SHELX 76, Program for Crystal Structure Determination, University of Cambridge, 1976.

19 G. M. Sheldrick, SHELXS 86, Program for Crystal Structure Determination, in *Crystallographic Computing 3*, eds. G. M. Sheldrick, C. Kruger and R. Goddard, Oxford University Press, 1985, p. 175.

20 C. K. Johnson, ORTEP, Report ORNL-3794, Oak Ridge National Laboratories, Oak Ridge, TN, 1965.

Received 14*th March* 1994; *Paper* 4/01504E